Materials and Structures, 1994, **27**, 563–571

Size effects on tensile fracture properties: a unified explanation based on disorder and fractality of concrete microstructure

ALBERTO CARPINTERI, GIUSEPPE FERRO

Politecnico di Torino, Dip. di Ingegneria Strutturale, 10129 Torino, Italy

Tests were carried out using three independent jacks orthogonally disposed, making it possible to apply a purely tensile force, so that the secondary flexural stresses, if kept under control, constitute a degree of error comparable with the values allowed for normal testing apparatus. The method enables a stress versus strain curve to be plotted with the descending (softening) branch up to the point where the cross-section of the tensile specimen breaks away. The principal purpose is to avoid any spurious effect that might provide a fallacious explanation of the recurring size effects on apparent tensile strength and fictitious fracture energy. Once the secondary effects have been excluded, only the disorder and fractality of the concrete microstructure remain to explain such fundamental trends. In the case of tensile strength, the dimensional decrement represents self-similar weakening of the material ligament, due to pores, voids, defects, cracks, aggregates, inclusions, etc. Analogously, in the case of fracture energy, the dimensional increment represents self-similar tortuosity of the fracture surface, as well as self-similar overlapping and distribution of microcracks in the direction orthogonal to that of the forming macrocrack.

1. INTRODUCTION

Robert L'Hermite, in his well known book of 1955 [1], considered the difficulties arising when a pure and objective tensile test on concrete is to be performed. Quoting from his work,

> 'Pour connaître la résistance du béton en traction, il reste donc l'essai direct, très peu employé à cause de sa difficulté de réalisation. En admettant que le centrage de l'effort soit fait avec toute la rigueur désirable, certains auteurs craignent que toute fissuration conduisant à une dissymétrie de la section entraîne la production d'un moment de flexion qui accélère la rupture. Ceci pourrait être la cause d'une diminution de la résistance apparente en traction.'

The study of the tensile properties of heterogeneous materials (concrete, mortar, rocks, etc.) has involved numerous researchers in recent years. Different test techniques were developed and several theories were formulated in support of the results obtained. The substantial difficulties that the tension test had to overcome are 1, to obtain a stable and complete post-peak softening response, and 2, to maintain always the tensile load perfectly centred so as to avoid the presence of bending moments which can alter the results.

The post-peak softening response can be obtained only if the loading process is deformation-controlled. Rusch and Hilsdorf [2] and then Hughes and Chapman [3] as well as Evans and Marathe [4] showed that the stress versus strain curve obtained from direct tension of concrete is similar to that obtained from compression even in the post-peak regime. The localization of strain in direct tensile tests on concrete was discussed by Heilmann, Hilsdorf and Finsterwalder [5]. Strain gauges were glued at different positions on a 600 mm long concrete specimen. The load was eccentrically applied in an attempt to produce stable fracture.

More recently, Petersson [6] carried out tensile tests in order to study the development of the fracture zone in concrete. The tests were performed in a very stiff tensile testing machine constituted by three aluminium columns with cylindrical heating elements. The aluminium columns expanded when they were heated and transmitted the tensile load to the specimen.

Gopalaratnam and Shah [7] proposed a test technique with a universal joint to minimize in-plane and out-of-plane bending effects and a particular wedge-type frictional grip system to assure that fracture occurred away from the grips. With this instrumentation they performed tests on constant size specimens and observed that the notches do not influence the average response of the specimens and that the tangent modulus of elasticity in tension is comparable with that in compression.

Reinhardt and co-workers [8] performed cyclic tests on notched specimens and proposed softening constitutive laws on the basis of their experimental results.

Phillips and Zhang [9] designed a stiff frame which proved highly effective in order to obtain stable and complete stress–deformation curves on both unnotched and notched plain concrete. They also established a substantial homogeneity in the behaviour of the notched specimens compared with that of the unnotched ones.

0025-5432/94

Van Mier [10] studied the problem of the influence of boundary rotation stiffness and indicated some conditions for test stability. Moreover, he described a vacuum impregnation experiment using a low viscosity fluorescing fluid which allows monitoring of the complete crack growth process. He could observe self-similar crack patterns, and Saouma *et al.* [11] emphasized the fractal nature of the concrete fracture surfaces.

A completely new testing apparatus made up of three mutually orthogonal actuators is proposed in the present paper. In this way, it is possible to perform a true direct tensile experiment on concrete, whereas usually tension and bending are both present. The principal purpose is that of avoiding any spurious effect that might provide a fallacious explanation of the basic size effects on apparent tensile strength and fictitious fracture energy. Once these secondary effects have been excluded, only the fractality [12, 13] of the heterogeneous microstructure remains to explain such fundamental trends.

2. DESCRIPTION OF SPECIMENS AND TEST EQUIPMENT

The first problem we were faced with was that of defining the shape and the size of the test specimens. The shape is linked to the choice of the type of gripping mechanism and to the desirability of creating a preferential fracture zone. The size of the test specimen is, instead, limited both by the size of the aggregate used (lower limit) and by the potentialities of the available equipment (upper limit). In an initial cycle of tests the approach was to use relatively small aggregates to make it possible to perform experiments on test specimens of varying sizes (Fig. 1). The test specimens were flared in the centre as shown in Fig. 1. The thickness of the test specimens, 10 cm, was maintained constant for the entire set, while the transverse dimension was 0.5, 1, 2, and 4 times that of the thickness.

The test specimen was glued to steel supporting plates for attachment to the load-bearing system. An epoxy resin based bicomponent adhesive was chosen. This ensures a high adherence both to concrete and to steel. The plates were secured to the lower and upper cross members with a series of bolts. The shape of the test specimen, the two ends of which had a cross-section three times larger than the cross-section undergoing tensile testing, made it possible to reduce the stress in the glued area.

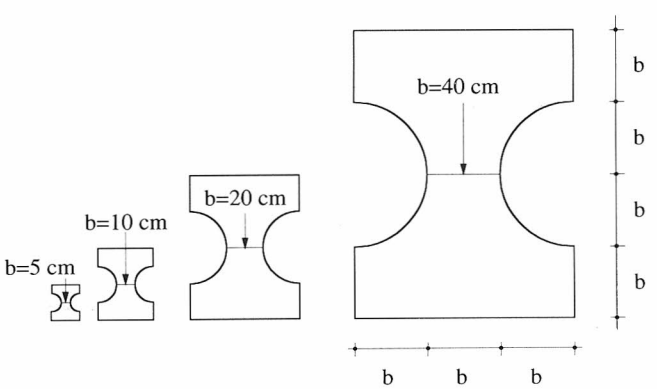

Fig. 1 Geometries of the specimens tested.

The testing method has been developed taking into account the following four factors: (i) the general impossibility of making geometrically perfect test specimens, since even if considerable care is taken in their preparation, they inevitably present certain defects in shape; (ii) the extreme difficulty of eliminating centring errors even if recourse is made to introducing hinges in the chain applying tensile force (it is by no means certain that the test specimen is coaxial with the hinges); (iii) even supposing that centring of the stress is performed as exactingly as possible, the development of cracks during the loading phase leads to a new cross-sectional asymmetry and hence produces a bending moment; and (iv) the use of closed-circuit electronically servo-controlled machines becomes indispensable in order to maintain a constant strain rate, and in order to detect the descending (softening) branch of the load–extension curve, measuring the extension by strain gauges (extensometers) directly applied to the test sample.

The procedure devised was to use servo-controlled machines to keep the flexural forces under control along two mutually orthogonal planes. For this purpose it was necessary to have some sort of electrical signal, capable of functioning as a control signal in a counter-reaction system, which was proportional to the bending moment developed on the specimen cross-section.

Initially the new counter-reaction signals were obtained by detecting the strains from electrical strain gauges set on two opposite sides of the specimen and connected onto the adjacent sides of the measuring bridge. In this way two electrical signals were obtained proportional to the difference in the strains and hence proportional to the bending moment acting along a plane passing through the axis of the specimen, each in the direction perpendicular to the faces of the specimen to which the strain gauges were attached. The test proved particularly useful for pinpointing the problems involved in the simultaneous operation of the three servomechanisms employed. It did not, however, prove satisfactory as regards the response curves, which still emerged as divergent (Fig. 2).

It thus appeared logical to use, for control purposes, the same analogue signals supplied by the four extensometers employed for measuring the strains, carrying out appropriate algebraical operations on them. If ϵ_1, ϵ_2, ϵ_3, ϵ_4 are the strains of the single measuring points set out as shown in Fig. 3, the strains due to bending moment turn out to be: along the x axis,

$$\epsilon_x = \frac{(\epsilon_2 + \epsilon_4) - (\epsilon_1 + \epsilon_3)}{2}$$

and along the y axis,

$$\epsilon_y = \frac{(\epsilon_1 + \epsilon_2) - (\epsilon_3 + \epsilon_4)}{2}$$

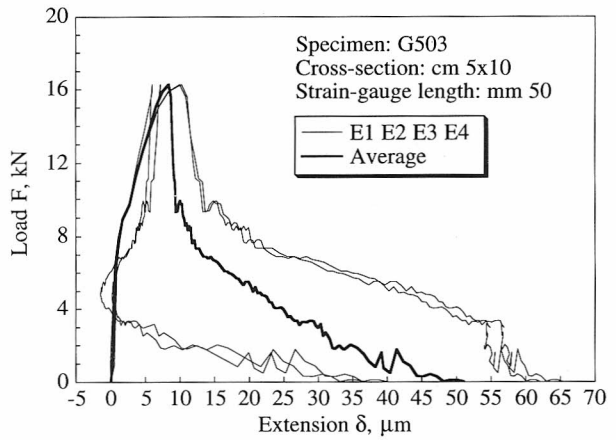

Fig. 2 Load versus extension diagrams coming from the four extensometers. Single jack solution.

Fig. 3 gives the electrical scheme illustrating the use of analogue amplifiers for performing operations of addition and subtraction of the four extensometers signals and how they are connected up to the three servocontrolled jacks.

Fig. 4 depicts the test scheme and shows the overall set-up of the equipment with one of the largest specimens under load. The central jack was suspended from the contrast structure via a ball joint and was connected again with a ball joint to the moveable cross-member. The jack applies the tensile force to the centre of the cross-member and, as already mentioned, the control is performed by summation of the signals from the four extensometers mounted on the specimen. The other two jacks are disposed one at the end of the main cross-member and the other at the end of an auxiliary cross-member set perpendicular to the main one. Both jacks generate a couple acting along a principal plane of the specimen (Fig. 5).

The test is thus carried out by the central jack imposing an extension on the specimen at a constant rate, while the other two jacks maintain the values ϵ_x and ϵ_y equal to zero. Fig. 6 presents the load–extension curves obtained with the three jack method, and it can be seen how they almost coincide up to the point where the load goes to zero in the softening phase.

3. EXPERIMENTAL RESULTS

The tests were carried out on four specimen sizes. The dimensions of the minimum cross-section of the smallest specimen were 5 cm × 10 cm, 10 cm × 10 cm for the second size, 20 cm × 10 cm for the third and 40 cm × 10 cm for the largest size (Fig. 1). Four specimens of each size were cast. The concrete mix had a water/cement ratio of 0.5. The maximum gravel size was d_{max} = 16 mm while the mean compression strength was f'_t = 36.9 MPa.

For the smallest size, only one complete diagram is available, in that the other three were used to set the sensitivity of the three servocontrolled machines. For the subsequent sizes, two complete diagrams are available. For the specimens of length 80 cm the hinges were introduced to bind the lower cross-head since, in the first two specimens, a failure near the grip plates had occurred. For this size only a complete curve is available. On the other hand, for the largest specimens only the values of the tensile strength are available, because the length of the extensometers (40 cm) was greater than the critical value and therefore snap-back behaviour occurred. The results of the tests are reported in Table 1.

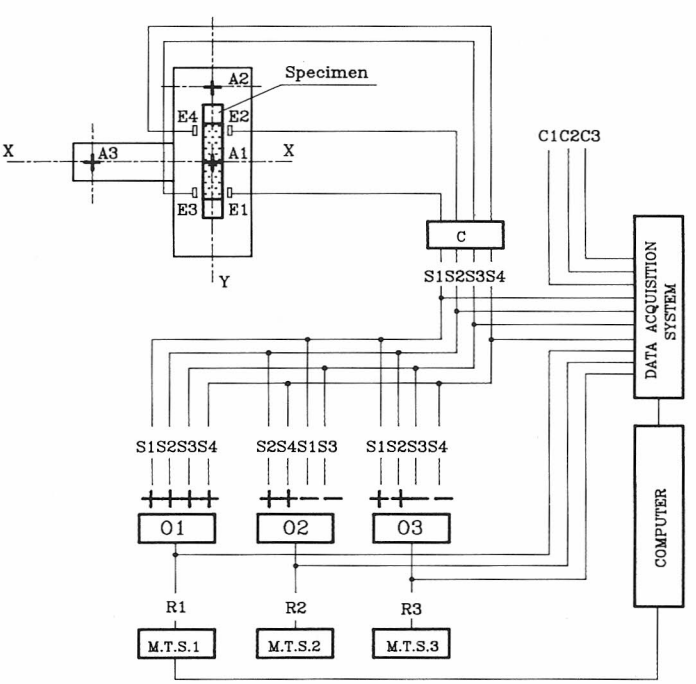

LEGEND :

E1 E2 E3 E4	Fracture mechanics extensometers
S1 S2 S3 S4	Extensometer output signals
A1	Actuator used to apply tension load
A2	Actuator used to reduce the bending moment in the Y–Y direction
A3	Actuator used to reduce the bending moment in the X–X direction
C	Signal conditioner amplifier
01	Operational amplifier for the addition of the four extensometer output signals
02 03	Operational amplifiers to make other algebraical operations on extensometer output signals
R1=S1+S2+S3+S4	Feed–back signal for actuator A1
R2=(S2+S4)−(S1+S3)	Feed–back signal for actuator A2
R3=(S1+S2)−(S3+S4)	Feed–back signal for actuator A3
C1 C2 C3	A1 A2 A3 actuator output signals

Fig. 3 Counter-reaction electrical system.

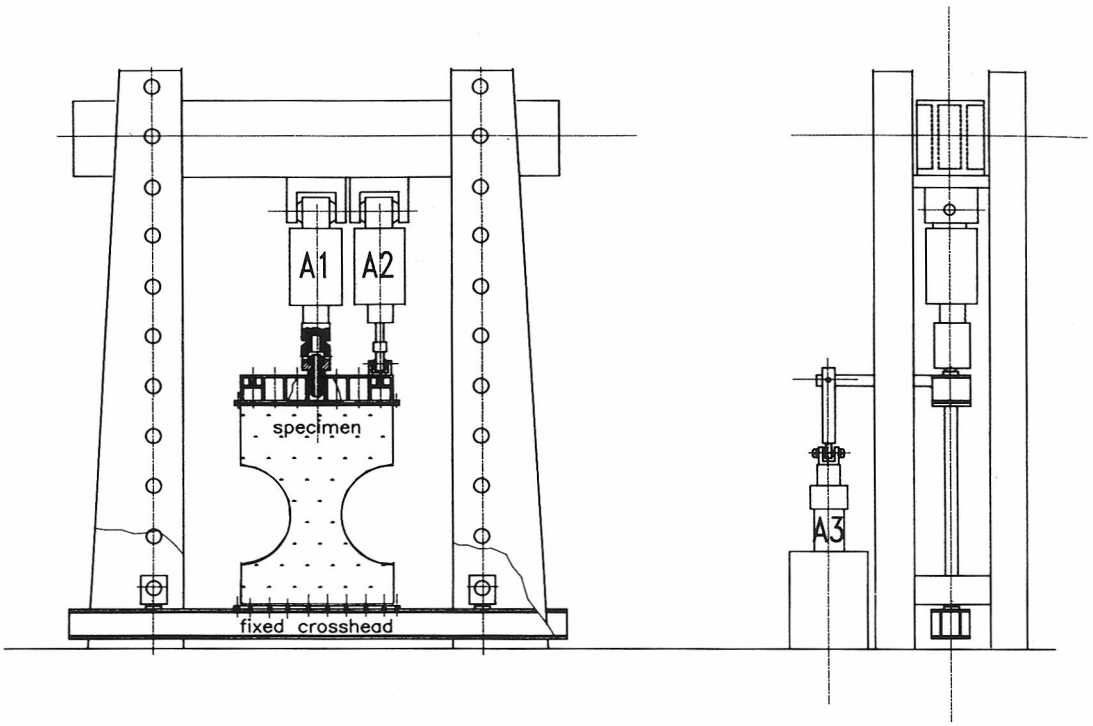

Fig. 4 Testing scheme with the three jack solution.

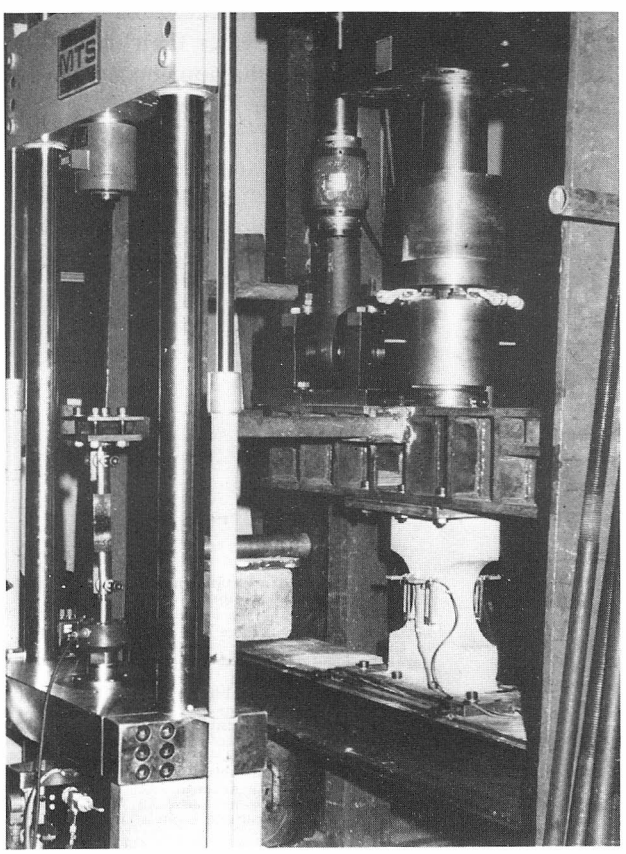

Fig. 5 Three jack solution.

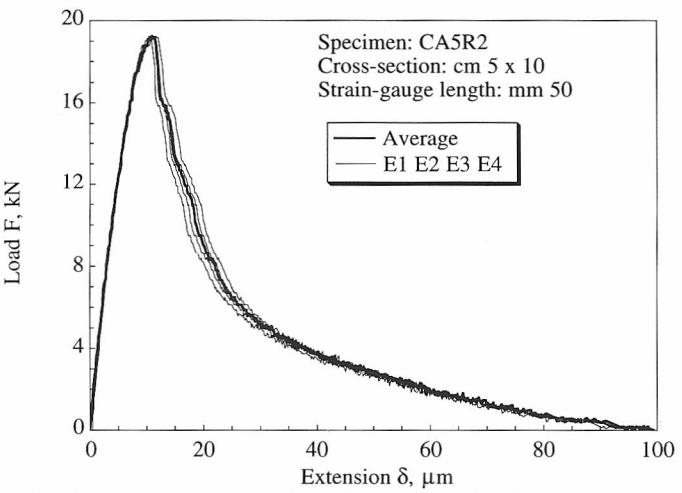

Fig. 6 Load versus extension diagrams coming from the four extensometers. Three jack solution.

Table 1 Experimental average values for tensile strength and fracture energy

Specimen width (cm)	Cross-sectional area (cm^2)	Tensile strength σ_u (MPa)	Fracture energy G_F (N/mm)
5	50	4.25	0.083
10	100	3.78	0.102
20	200	3.64	0.142
40	400	3.11	—

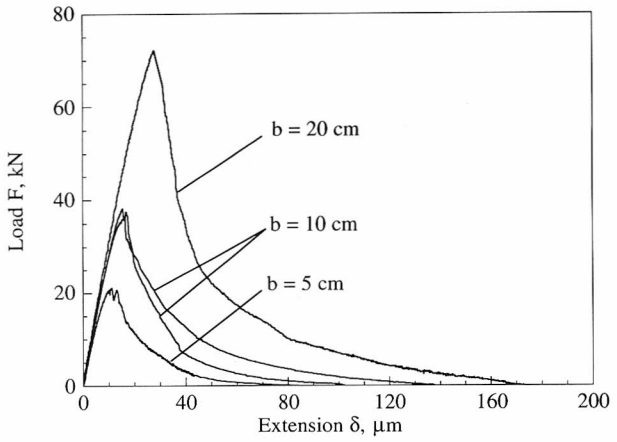

Fig. 7 Experimental load versus extension curves obtained from three different specimen sizes.

The experimental load versus extension curves for the three specimen sizes are shown in Fig. 7. It is important to note how the slope of the elastic portion is the same for all sizes. This is due to the fact that the lengths of the extensometers were proportional to the size of the specimens (5 cm for the smallest ones, 10 cm and 20 cm for the other two). Moreover, the shape of these curves is in any case the same and this fact means that this kind of test procedure is independent of the machine stiffness. In fact, unlike the results reported by Van Mier [10] for the specimens tested with fixed grip plates, no bumps were found. This is due to the load, which is always centred when the control takes place both in-plane and out-of-plane. In the tests discussed by Van Mier, on the other hand, the check was only in the specimen plane, and no check was performed for the out-of-plane eccentricity.

The values of the apparent tensile strength are plotted in Fig. 8 against the specimen size in a bilogarithmic plane. The size effect is represented by the slope of the linear regression of the points of the diagram. It is evident how the tensile strength decreases with increasing specimen size. The fracture energy instead shows the opposite trend: i.e., it increases with specimen size. The values obtained experimentally are reported in Fig. 9 on the bilogarithmic plane ln G_F versus ln b. The variation

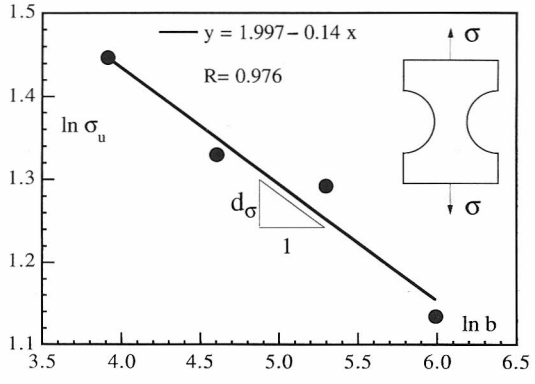

Fig. 8 Size effect on apparent tensile strength.

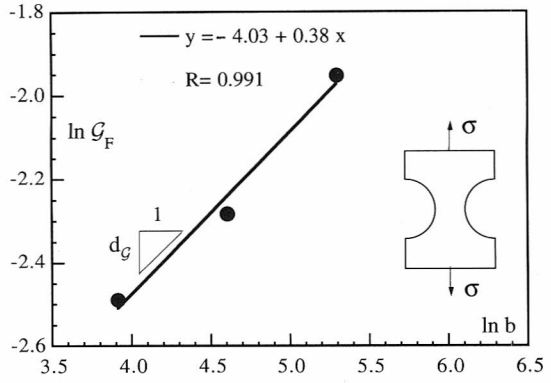

Fig. 9 Size effect on fictitious fracture energy.

of G_F as a function of size is represented by the slope of the linear regression diagram.

4. FRACTAL NATURE OF MATERIAL LIGAMENT AND SIZE EFFECTS ON NOMINAL TENSILE STRENGTH

It is well known that the nominal tensile strength of many materials undergoes very clear size effects. The usual trend is that of a strength decrease with size, and this is more evident for disordered (i.e. macroscopically heterogeneous and/or damaged) materials. Griffith [14] explained the strength size effect in the case of glass filaments, assuming the existence of inherent microcracks of a size proportional to the filament cross-section diameter. Some years later Weibull [15] gave a purely statistical explanation of the same phenomenon accordng to the weakest-link-in-a-chain concept. Only recently have the two views been harmonized, enriching the empirical approach of Weibull with the phenomenological assumption of Griffith [16–18]. A *statistical size distribution of self-similarity* may be defined [18, 19] for which the most dangerous defect proves to be of a size proportional to the structural size. This corresponds to materials presenting a considerable dispersion in statistical microcrack size distribution (disordered materials). In this case, the power of the LEFM stress singularity, $\frac{1}{2}$, turns out to be the slope of the strength versus size decrease in a bilogarithmic diagram. When the statistical dispersion is relatively low (ordered materials) the slope is less than $\frac{1}{2}$, and tends to zero for regular distributions (perfectly ordered materials).

Although the above contains the fractal concept of self-similarity, this is circumscribed only to the defect of maximum size, whereas the disordered nature of the material microstructure is completely disregarded. The real nature of the material will be described herein by a more complex fractal model, where the property of self-similarity is extended to the whole defect population. This model represents a closer picture of reality and is consistent with the fractal explanation of the fracture energy size effect, which will be proposed in the next section. On the other hand, as will be shown, slope values higher than $\frac{1}{2}$ would represent, with both models, a

degree of disorder that is so high as to be absent usually in real materials.

Let us assume that the reacting section or ligament of a disordered material at peak stress could be represented as a fractal space of dimension $\alpha = 2 - d_\sigma$, with $1 < \alpha \leq 2$ and, therefore, $0 \leq d_\sigma < 1$. The dimensional decrement d_σ may be due to the presence of cracks and voids and then, generally, to a cross-sectional weakening.

Let us consider two bodies, geometrically similar and made up of the same disordered material. If the ratio of geometrical similitude is equal to b and the *renormalized tensile strength* σ_u^* is assumed to be a material constant and to have the physical dimensions [force] × [length]$^{-(2-d_\sigma)}$, we have:

$$\sigma_u^* = \frac{F_1}{1^{2-d_\sigma}} = \frac{F_2}{b^{2-d_\sigma}} \tag{1}$$

F_1 and F_2 being the ultimate tensile forces acting on the two bodies, respectively.

On the other hand, the apparent nominal tensile strengths are, respectively,

$$\sigma_u^{(1)} = \frac{F_1}{1^2}, \qquad \sigma_u^{(2)} = \frac{F_2}{b^2} \tag{2}$$

where the latter, according to (1), becomes

$$\sigma_u^{(2)} = \sigma_u^{(1)} b^{-d_\sigma} \tag{3}$$

We can write the relationship between nominal strengths related to different sizes in logarithmic form:

$$\ln \sigma_u = \ln \sigma_u^{(1)} - d_\sigma \ln b. \tag{4}$$

Equation 4 represents a straight line with slope $-d_\sigma$ in the $\ln \sigma_u$ versus $\ln b$ plane (Fig. 8).

Confirmation of (4) has been provided by several previous investigations, carried out on different metallic or cementitious materials and with different specimen geometries: tension, bending, Brazilian, etc. These results were summarized by Carpinteri [18, 19]. The same trends have been found also in the present experimental program aimed at evaluating the true tensile properties of concrete. As may be seen from Fig. 8, the slope of the strength decrease proves to be equal to 0.14, thus revealing a material ligament of dimension 1.86, i.e., a fractal set which is very close to a 2-dimensional surface. If the force is assumed as sustained by a ligament of dimension 1.86, a constant (universal) strength parameter may be measured (Fig. 10). The fractal nature of the material ligament emerges very clearly at the size scales of the specimens. On the other hand, the property of self-similarity is very likely to vanish or change at higher or lower scales, owing to the limited character of the particle size curve.

5. FRACTAL NATURE OF FRACTURE SURFACE AND SIZE EFFECTS ON FICTITIOUS FRACTURE ENERGY

The fracture surfaces of metals [20] and concrete [11] present a fractal nature with a roughness producing a

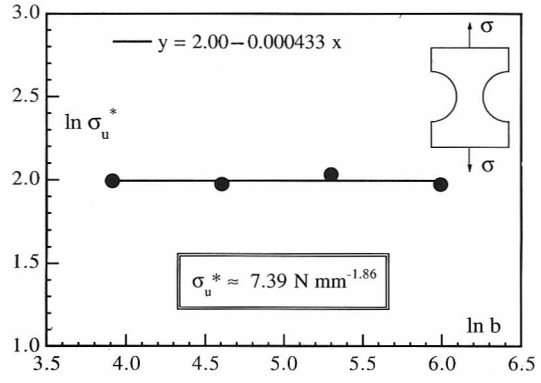

Fig. 10 Renormalized value of tensile strength.

dimensional increment with respect to the number 2. Even in this case we can detect an evident mechanical consequence, considering the size effects on fracture energy G_F. Since Hillerborg's proposal for a concrete fracture test was published as a RILEM Recommendation [21], several researchers have measured a fracture energy G_F which increases with the specimen sizes and, more specifically, with the size of the uncracked ligament. Such a trend has been found systematically, and in each case the authors of the papers describing these experiments have tried to provide various empirical or phenomenological explanations, without, however, endeavouring to interpret their findings in a larger conceptual framework. On the other hand, if we wish to understand the experimental observations, it is necessary to abandon the classical thermodynamic concept of surface energy of an ideal solid, and to assume the energy dissipation to be occurring in a fractal space of dimension $\alpha = 2 + d_G$, with $2 \leq \alpha < 3$ and, therefore, $0 \leq d_G < 1$. This represents an attenuation of fracture localization due to material heterogeneity and multiple cracking.

Let us consider two bodies, geometrically similar and made up of the same disordered material. If the ratio of geometrical similitude is equal to b and the *renormalized fracture energy* G_F^* is assumed to be a material constant and to have the physical dimensions [force] × [length]$^{-(2+d_G)}$, we obtain:

$$G_F^* = \frac{E_1}{1^{2+d_G}} = \frac{E_2}{b^{2+d_G}}, \tag{5}$$

E_1 and E_2 being the energies dissipated in the two bodies, respectively. On the other hand, the apparent fracture energies are, respectively,

$$G_F^{(1)} = \frac{E_1}{1^2}, \qquad G_F^{(2)} = \frac{E_2}{b^2} \tag{6}$$

where the latter, according to (5), becomes

$$G_F^{(2)} = G_F^{(1)} b^{d_G}. \tag{7}$$

We can write the relationship between fracture energies related to different sizes in logarithmic form:

$$\ln G_F = \ln G_F^{(1)} + d_G \ln b. \tag{8}$$

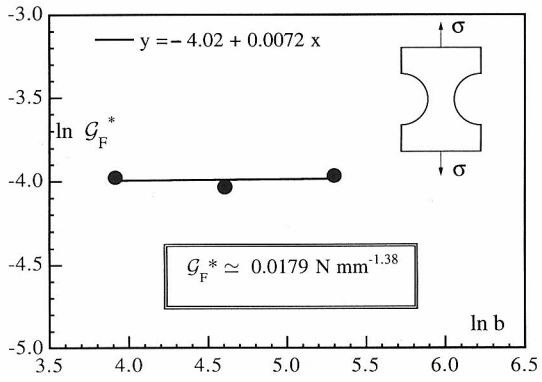

Fig. 11 Renormalized value of fracture energy.

Equation 8 represents a straight line with slope d_G in the ln G_F versus ln b plane (Fig. 9).

The same trends have been found in the present experimental investigation. Tensile testing performed at the Politecnico di Torino provides a plot slope equal to 0.38 (Fig. 9), which allows a constant (universal) energy parameter to be obtained in the case where the dissipation is considered as occurring in a damaged space of dimension 2.38 (Fig. 11).

6. CONCLUSIONS

The abundant literature on tensile strength and fracture energy size effects as well as the newly introduced fractal theories would appear to indicate the need for a dramatic change in the conceptual framework and even in our whole way of thinking, if we want to consider and measure material constants in materials engineering and in fracture mechanics. This means that we have to give up ideal reference areas when we consider the tensile strength and fracture energy of disordered materials with a fractal microstructure. The so-called homogeneous materials (on the macroscopic scale or macrolevel) present, on the other hand, a very small deviation from the ideal case. Only on the microscopic scale or microlevel might they present a higher degree of fractality [22]. For concrete and rocks, for which the micro- and mesolevels coincide with the structural level, the tensile strength is given by a force acting on a surface having a fractal dimension lower than 2, and also the fracture energy is represented by a dissipation over a surface with a fractal dimension higher than 2.

In the case of tensile strength the dimensional decrement represents self-similar weakening of the reacting cross-section or ligament, due to pores, voids, defects, cracks, aggregates, inclusions, etc. Likewise, in the case of fracture energy, the dimensional increment represents self-similar tortuosity of the fracture surface, due to aggregates and inclusions, as well as self-similar microcrack overlapping and distribution even in the direction orthogonal to that of the developing macrocrack [10].

As regards the dimensional decrement d_σ and the dimensional increment d_G, experimentally they appear always contained in the interval $[0, \frac{1}{2}]$. The dimensional decrement d_σ tends to the LEFM limit $\frac{1}{2}$ only for extremely brittle and disordered materials (defect size distribution of self-similarity) and is connected to the Weibull parameter m in the case of planar similitude [18, 19]:

$$d_\sigma = \frac{2}{m} \tag{9}$$

Even the dimensional increment d_G tends to the same limit $\frac{1}{2}$ for extremely brittle and disordered materials. The explanation for the latter bound could arise for dimensional analysis reasons. A generalization of the *brittleness number* defined by the first author [23–28] could in fact be the following:

$$s_E^* = \frac{G_F^*}{\sigma_u^* b^{(1-d_\sigma-d_G)}} \tag{10}$$

If we postulate that the reversal of the physical roles of toughness and strength is absurd, the exponent of the characteristic linear size b must be positive:

$$d_\sigma + d_G < 1. \tag{11}$$

The sum of the dimensional decrement (for a material ligament) and the dimensional increment (for a fracture surface) must therefore be lower than unity. On the other hand, when, for very disordered materials, we have $d_\sigma \simeq \frac{1}{2}$, the upper bound of 11 becomes $d_G \lesssim \frac{1}{2}$.

The above fractal interpretations could be regarded by some as purely mathematical abstractions, if not indeed distortions of reality. The truth is that both classical geometrical domains and fractal geometrical loci are idealizations of reality. The question that should be answered is the following: which model is closer to a real fracture trajectory in a concrete specimen: a straight line or the von Koch curve? Of course the latter, even though the fractal nature of the fracture trajectory is random and valid only in a limited scale range. This means that, for size scales tending to infinity or, in other words, for very large specimens, tensile strength σ_u and fracture energy G_F may appear constant by varying the specimen size [29, 30], whereas, for size scales where random self-similarity holds, the so-called 'universal properties' of the system (σ_u^*, G_F^*) are constant, although they are represented by physical quantities with unusual dimensions. The last result represents the target of the so-called 'renormalization' procedure, i.e., the determination of physical quantities that are invariant under a change of length scale [31, 32].

ACKNOWLEDGEMENTS

The present research was carried out with the financial support of the Ministry of University and Scientific Research (MURST) and the National Research Council (CNR).

REFERENCES

1. L'Hermite, R., 'Idées actuelles sur la technologie du béton', Collection de l'Institut Technique du Bâtiment et des Travaux Publics, Paris, 1955.

2. Rusch, H. and Hilsdorf, H. K., 'Deformation characteristics of concrete under axial tension', *Voruntersuchungen* **44** (1963).
3. Hughes, B. P. and Chapman, G. P., 'The complete stress–strain curves for concrete in direct tension', *RILEM Bull.* **30** (1966) 95–97.
4. Evans, R. H. and Marathe, M. S., 'Microcracking and stress–strain curves for concrete in tension', *Mater. Struct.* **1** (1968) 61–64.
5. Heilmann, H. G., Hilsdorf, H. K. and Finsterwalder, K., 'Festigkeit und Verformung von Beton unter Zugspannungen', *Deutsch. Ausschuss Stahlbeton* **203** (1969).
6. Petersson, P. E., 'Crack growth and development of fracture zones in plain concrete and similar materials', Report TVBM-1006 (Division of Building Materials, Lund Institute of Technology, 1981).
7. Gopalaratnam, V. S. and Shah, S. P., 'Softening response of plain concrete in direct tension', *J. ACI* **82** (1985) 310–323.
8. Reinhardt, H. W., Cornelissen, A. W. and Hordijk, D. A., 'Tensile tests and failure analysis of concrete', *J. Struct. Eng.* **112** (1986) 2462–2477.
9. Phillips, D. V. and Zhang, B., 'Fracture energy and brittleness of plain concrete specimens under direct tension', in 'Fracture Behaviour and Design of Materials and Structures', edited by D. Firrao, Proceedings of the 8th European Conference on Fracture, Torino, Italia, October, 1990 (EMAS, Warley, 1991) pp. 646–652.
10. van Mier, J. G. M., 'Scaling in tensile and compressive fracture of concrete', in 'Applications of Fracture Mechanics to Reinforced Concrete', edited by A. Carpinteri (Chapman and Hall, London, 1992) pp. 19–31.
11. Saouma, V. E., Barton, C. C. and Gamaleldin, N. A., 'Fractal characterization of fracture surfaces in concrete', *Engng Fract. Mech.* **35** (1990) 47–53.
12. Mandelbrot, B. B., 'The Fractal Geometry of Nature' (W.H. Freeman and Company, New York, 1982).
13. Falconer, K., 'Fractal Geometry: Mathematical Foundations and Applications' (Wiley, Chichester, 1990).
14. Griffith, A. A., 'The phenomena of rupture and flow in solids', *Phil. Trans. R. Soc. Lond.* **A221** (1921) 163–198.
15. Weibull, W., 'A Statistical Theory of the Strength of Materials' (Swedish Royal Institute for Engineering Research, Stockholm, 1939).
16. Freudenthal, A. M., 'Statistical approach to brittle fracture', in 'Fracture' edited by H. Liebowitz, Vol. 2 (Academic Press, New York, 1968) pp. 591–619.
17. Jayatilaka, A. S., 'Fracture of Engineering Brittle Materials' (Applied Science, London, 1979).
18. Carpinteri, A., 'Decrease of apparent tensile and bending strength with specimen size: two different explanations based on fracture mechanics', *Int. J. Solids Struct.* **25** (1989) 407–429.
19. *Idem* 'Mechanical Damage and Crack Growth in Concrete: Plastic Collapse to Brittle Fracture' (Martinus Nijhoff, Dordrecht, 1986).
20. Mandelbrot, B. B., Passoja, D. E. and Paullay, A. J., 'Fractal character of fracture surfaces of metals', *Nature* **308** (1984) 721–722.
21. RILEM Technical Committee 50, 'Determination of the fracture energy of mortar and concrete by means of three-point bend tests on notched beams', Draft Recommendation, *Mater. Struct.* **18** (1985) 287–290.
22. Meakin, P., 'Models for material failure and deformation', *Science* **252** (1991) 226–234.
23. Carpinteri, A., 'Experimental determination of fracture toughness parameters K_{IC} and J_{IC} for aggregative materials', Proceedings of the Fifth International Conference on Fracture (Pergamon Press, Oxford, 1981) pp. 1491–1498.
24. *Idem*, 'Static and energetic fracture parameters for rocks and concretes', *Mater. Struct.* **14** (1981) 151–162.
25. *Idem*, 'Notch sensitivity in fracture testing of aggregative materials', *Engng Fract. Mech.* **16** (1982) 467–481.
26. *Idem*, 'Interpretation of the Griffith instability as a bifurcation of the global equilibrium', in 'Applications of Fracture Mechanics to Cementitious Composites', edited by S. P. Shah (Martinus Nijhoff, Dordrecht, 1985), pp. 287–316.
27. *Idem*, 'Limit analysis for elastic-softening structures: scale and slenderness influence on the global brittleness', in 'Brittle Matrix Composites', edited by A. M. Brandt and I. H. Marshall (Elsevier Applied Science, London, 1986) pp. 497–508.
28. *Idem.*, 'Cusp catastrophe interpretation of fracture instability', *J. Mech. Phys. Solids* **37** (1989) 567–582.
29. Tang, T., Shah, S. P. and Ouyang, C., 'Fracture mechanics and size effect of concrete in tension', *J. Struct. Engng, ASCE* **118** (1992) 3169–3185.
30. Lange, D. A., Jennings, H. M. and Shah, S. P., 'Relationship between fracture surface roughness and fracture behavior of cement paste and mortar', *J. Am. Ceram. Soc.* **76** (1993) 589–597.
31. Wilson, K. G., 'Renormalization group and critical phenomena', *Phys. Rev.* **B4** (1971) 3174–3205.
32. Herrmann, H. J. and Roux, S., 'Statistical Models for the Fracture of Disordered Media' (North-Holland, Amsterdam, 1990).

RESUME

Effets d'échelle sur les propriétés de la rupture en traction: explication unitaire basée sur le désordre et le caractère fractal de la microstructure

L'expérience a été conduite en utilisant trois vérins indépendants placés orthogonalement. Celà a permis d'appliquer une charge de traction pure de façon que les contraintes secondaires de fléxion, si elles sont contrôlées, donnent des erreurs dont l'ordre de grandeur est comparable au valeurs tolérées pour les appareils utilisés normalement. Ce gendre de méthode expérimentale permet de suivre la partie descendante (écrouissage négatif) de la courbe effort–déformation jusqu'au point où la section transversale de l'échantillon sous traction se casse. Le but principal est d'éviter tous les faux effets qui peuvent nous conduire à des explications erronées à propos des effets d'échelle récurrents sur l'allure de la résistance à la traction apparente et de l'énergie de rupture fictive. Une fois que les effets secondaires ont été exclus, seuls le désordre et le caractère fractal de la microstructure du béton permettent de justifier cette tendance fondamentale. Dans le cas de la résistance à la traction, la diminution dimensionnelle représente un affaiblissement des liaisons du matériau, dû aux pores, aux vides, aux défauts, aux fissures, aux granulats, aux inclusions, etc. D'une manière analogue, dans le cas de l'énergie de rupture, l'accroissement dimensionnel représente la sinuosité de la surface de rupture, ainsi que la superposition et la distribution des microfissures dans la direction perpendiculaire à celle des microfissures en formation.